DSSE in European-Type Networks Using PLC-Based Advanced Metering Infrastructure

Mahmoud Rashad Ahmed ⓘ, José M. Cano ⓘ, *Senior Member, IEEE*, Pablo Arboleya ⓘ, *Senior Member, IEEE*, Lucía Suárez Ramón, and Almoataz Y. Abdelaziz ⓘ, *Senior Member, IEEE*

Abstract—This paper addresses the problem of real-time state estimation in European-type four-wire low-voltage distribution networks with advanced metering infrastructure based on power line communication (PLC). The main drawback of this type of infrastructure is its high latency and a sequential data sampling process. Both factors make it difficult to obtain instantaneous values from the smart meters in a timely and adequate manner to estimate the real-time state of the system. This problem may be solved in the future with the deployment of metering systems based on other technologies such as 5G. However, PLC technology prevails in many countries, and is not likely to be replaced in the medium term. In the meantime, a solution is needed to provide acceptable real-time state estimates in low voltage networks, not to hinder the active management of these assets in the context of smart grids. In this work, a solution is proposed that allows estimating the state of the low voltage network with a reasonable accuracy considering the low quality of the measurements provided by the deployed infrastructure. The system is validated using a portion of a real pilot network located in the north of Spain fed by a transformer station with seven feeders.

Index Terms—Advanced metering infrastructure, power line communication, real-time state estimation, smart meters.

NOMENCLATURE

Acronyms

AAE	Average absolute error
AMI	Advanced metering infrastructure
DCU	Data concentrator unit
DG	Distributed generation
DS	Distribution system
DSO	Distribution system operator
DSSE	Distribution system state estimation
DT	Distribution transformer
EMS	Energy management system
LAV	Least absolute value estimator
LNR	Largest normalized residual
LV	Low voltage
LVDS	Low voltage distribution system
MAE	Maximum absolute error
MV	Medium voltage
OD	Out of date
PLC	Power line communication
PF	Power flow
PMU	Phasor measurements unit
PS	Projection statistics
PV	Photovoltaic
RMSE	Root mean square error
RTC	Real-time clock
SCADA	Supervisory control and data acquisition
SG	Smart grid
SHGM	Schweppe Hubber Generalized M estimator
SM	Smart meter
SV	State variables
SyM-WLS	Synthetic measurements based WLS
TS	Transformer supervisor
TSSE	Transmission system state estimation
WLAV	Weighted Least Absolute Value estimator
WLS	Weighted least squares

Variables

$dist$	Distance of distribution line in meters
dWF	De-weighting factor
$J(\mathbf{x})$	Objective function
Q_f	Reactive power flow
Q_{inj}	Reactive power injection
P_f	Active power flow
P_{inj}	Active power injection
R	Distribution line resistance
STD_s	Standard deviation of the fitting process
T_i	Timestamp of the instantaneous i^{th} Measurement
T_s	Timestamp of the last instantaneous updated TS measurement
V	Voltage magnitude
X	Distribution line reactance
x_i^{est}	Estimated voltage magnitude in pu or angle in deg
x_i^{true}	True voltage magnitude in pu or angle in deg

Mahmoud Rashad Ahmed, José M. Cano, and Pablo Arboleya are with the Department of Electrical Engineering, University of Oviedo, 30013 Gijón, Asturias, Spain (e-mail: uo278851@uniovi.es; jmcano@uniovi.es; arboleya-pablo@uniovi.es).

Lucía Suárez Ramón is with the E-REDES (EDP Group), 33007 Oviedo, Spain (e-mail: lucias@edpenergia.es).

Almoataz Y. Abdelaziz is with the Electrical Power and Machines Department, Faculty of Engineering, Ain Shams University, Cairo 11517, Egypt (e-mail: almoatazabdelaziz@hotmail.com).

Y_s	Expected delay of a smart meter
Y_s^{est}	Random estimate of the time delay of a SM
β	An estimate for the median of pairwise sums
χ	Chi-square statistics
$\mathcal{L}$	Lagrangian function
ω	Weight factor
σ	Standard deviation of error
θ	Voltage phase angle

Vectors

$\mathbf{c(x)}$	Vector of virtual measurements functions
$\mathbf{e}$	Error vector
$\mathbf{h(x)}$	Vector of regular measurements functions
$\mathbf{r}$	Residual vector
$\mathbf{x}$	State vector
$\mathbf{z}$	Regular measurements vector
λ	Vector of Lagrange multipliers for virtual measurements
$\boldsymbol{\mu}$	Vector of Lagrange multipliers for regular measurements

Matrices

C	Jacobian of virtual measurements
H	Jacobian of regular measurements
$\hat{H}$	Weighted Jacobian of regular measurements

I. INTRODUCTION

ALTHOUGH TSSE is widely used since the 1970s [1], DSSE still faces some challenges. The LVDSs are the crucial parts of the application developments employed in SGs. DSSE is the core of most of these sophisticated applications in EMS. To fulfil the requirements of deploying the SG at a large scale, the DSSE must be able to carry out two main tasks: 1) merging measurement data with various qualities to achieve an accurate state estimate and 2) manipulate the huge number of measurement data transmitted by meter devices [2].

The usage of the DSSE in distribution networks has been belated because of two factors: the first was the lack of prevalent measurements in distribution systems and the second is the weak requirement for active management of the distribution network. In recent years, SMs are being installed down to the consumer level making the network more visible and that became a strategy followed in all countries of the European Union [3]. In the present, for effective SG deployment, DSSE is necessary to provide the vital information for different active and advanced applications such as, but not limited to, real-time monitoring and control, enabling the full capacity of DTs, voltage regulation, feeder reconfiguration and restoration along with DG, demand response, capacitor switching [4], [5].

Even though SMs have recently been massively deployed, the feasibility of DSSE in LVDS is still unclear due to the non-synchronized measurements provided by these devices. Despite the fact that the SM has a RTC which updates its time periodically [6], [7], the packet losses, performance deterioration, latency, and signal interference are examples of the consequences of the diverse spectrum characteristics of the crowded communications [8]. This, in turn, diminishes the communication performance of AMI which contains a great number of SMs, many access points, and a mesh network. This leads to a significant time delay, especially in case of PLC, due to the inherent sequential behavior of the communication between the SMs and the DCU [9].

Furthermore, since synchronizing the measurements of a big number of SMs is too costly to be applied in LVDS and may not be taken into account by many DSOs [9], [10], SMs may be programmed so as to send the measurements data at a specific time once per the day for billing purpose, which reduces the benefit of using real-time measurements of SMs [11], [12]. SM measurements are, as a base, non-synchronized due to errors in the adjustment of the RTC recording the time of measurements, and due to time delay of data transmission by narrow-band communication channels [7]. Thus, it is unfeasible to run a DSSE algorithm based on an instantaneous snapshot of the complete distribution network. Instead, DSSE may be executed using a set of measurements many of which are delayed by some time from a few seconds to several minutes.

Alternatively, using micro-PMUs, which can be installed at the DS level, is a suggested solution to the delays introduced by AMI. However, the deployment of such devices faces significant barriers like the high cost of these devices and its associated infrastructure [13]. Moreover, the use of micro-PMU in the SM is very far from the actual situation in Europe in the short or mid-term. Thus, it is important to deal with the problem with the current infrastructure.

Up to now, in contrast to many articles studying the impact of the time-delayed measurements of PMUs on the TSSE such as [14], little work can be found in literature regarding to the usage DSSE based on real-time measurements of SMs. According to [15], a WLS based DSSE is proposed utilizing a combination of PMUs and SMs using a genetic algorithm as an optimization method to achieve a trade-off between the economic implementation and the desired accuracy considering all SMs to have the same error 10%; however, the authors did not take into account the non-synchronized features of SM measurements compared to PMUs in [14]. Also, only a 50% uncertainty was assigned to the pseudo measurements used in [15] instead of accounting for short-term load variation profile.

To study the impact of using pseudo measurements in case of losing measurements of some SMs on the accuracy of DSSE in LVDS, the paper in [16] discussed specific conditions considering the observability and accuracy based on different combination of the instantaneous measurements of voltage magnitude, active and reactive power injection of SMs. The authors found that the best accuracy in estimating the voltage magnitude and angles at all nodes is achieved with the combination of these three magnitudes. Furthermore, the accuracy decreased linearly once losing more than one measurement until reaching the case of unobservabilty and it deteriorated more for missing measurements at nodes with high loads or PV systems. Neither the non-synchronized features of SMs nor the short-term load variation of historical pattern have been taken into account during the study.

In [17], [18], a DSSE for low voltage networks with DG was established and verified to check the technical feasibility of using SM measurements in LVDS for the purpose of observability and controllability. The DSSE uses calculated PF measurements at

load nodes, which are considered as pseudo measurements with 25-50% accuracy alongside with real-time voltage magnitude measurements; however, the latter measurements are treated without considering time delay. Moreover, the simulation in [17] is carried out on a balanced scenario and is not extended to the case of unbalanced three-phase loads.

Connecting large number of SMs, located at consumer nodes, with DCUs through limited PLC communication may lead to slow update rates [19]. To take communication latency into account, the confidence of the SM measurements is reduced in proportion to their time delay [10]. Practically, a snapshot estimation is difficult in case of considering real-time SM measurements. This enforces, DSOs to replace real-time SM measurements in some cases by so-called pseudo-measurements, developed based on historical SM readings with high variance, resulting in less accurate estimations [20].

Recently, an oriented work, as in [9] and [21], is presented to treat that issue. The first reference suggested using the idle time of the reading cycle of DCU to feed the DSSE with real-time SM measurements considering a trade-off between the accuracy and executing timeliness of DSSE. However, the latter proposed an approach to substitute the missing and the non-synchronized measurements of SM using Kalman smoother before inserting them to a robust DSSE able to discard the bad data of SMs.

Since this issue is still unclear, in-depth investigation is needed to reach the optimal recognition. So, this paper is a contribution to problems with the time-delayed measurements of SM in the European PLC based AMI, where the proposed approach uses a DSSE algorithm based on equality-constrained WLS in the form of the augmented matrix method. The key contributions in this paper are:

1) A novel time-delay emulator based on actual data obtained from a DSO has been developed. It generates time delays for each SM including some randomness using a Gaussian distribution with experimental statistical basis.

2) A new set of angle constraints for phase *b* and *c* of voltage phase angles is added in the proposed DSSE to match the reference angles of phase *b* and *c* of the voltage angles at the slack bus.

3) A modified PS version based DSSE, dedicated to unbalanced three-phase 4 wire DS, is implemented based on a real European distribution substation, in which the performance of the proposed method is validated by comparing it against two other DSSE alternatives found in literature.

The remainder of the paper is organized as follows. In Section II, the problem formulation is described. Section III explains the DSSE methodology, while Section IV introduces the proposal. Then, a case study is presented in Section V. Finally, in Section VI, the outcome and conclusion are summarized and future work is suggested.

II. PROBLEM STATEMENT

The typical SM used by European utilities is able to record the electrical consumption at given intervals, e.g. every 15, 30 or 60 minutes. In addition to electrical consumption data, the SM is also able to provide instantaneous measurements of voltage,
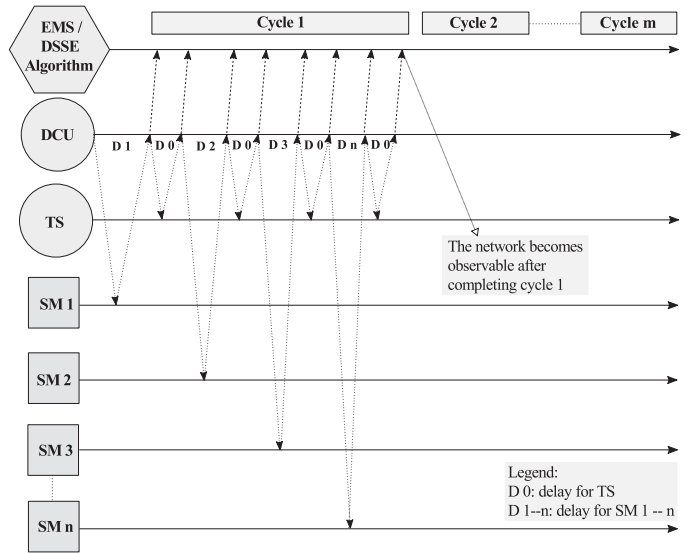

Fig. 1. A clarification for TS and SMs data access by EMS.

current, and power owing to its appealing functionality [6]. Instantaneous measurements correspond to real-time values are more precise than recorded ones. In fact, the latter are reports of average values through the total time interval of recording. The PLC communication is the preferred one among many other types in the LVDS because of its cost-effectiveness. However, its immunity to the attenuation and noise is very weak and can be influenced by long distance from the SM to DCU according to [22].

It is obvious that instantaneous measurements of SM are not synchronized and some delay arises when receiving these measurements [4] and [23]. In order to illustrate the causes of this delay, Fig. 1 shows the sequential transmitting and receiving of data as a repeating cycle between the DCU and SMs considering PLC as the communication media. The DCU typically transmits data via 4 G wireless technology to the EMS to be used by the DSSE algorithm.

Many factors can affect the speed of PLC communication [24], for instance, phase factor. Actually, the request for SM readings are usually conducted in a single phase, and those SMs connected to that phase tend to respond faster. Other factors that may influence communication speed are the distance (line impedance) from SM location to DCU, wiring connections and also electromagnetic compatibility, especially in zones with a lot of power converters (e.g. locations with a high penetration of PV generation).

In this study, only two factors are explicitly considered: phase factor and distance factor. Indeed, these two factors allow to capture most of the variability of the time response. The rest (including noise) are treated through a purely random perspective. The two former factors are employed based on communication delay statistics taken from a DSO company in Spain. The reading sequence of SMs by the DCU is assumed to be arbitrary, though other possibilities will be further investigated in a future study.

As all load/generator buses in SGs are equipped with SMs, power injections, P_{inj} and Q_{inj}, at these buses are available, together with the voltage magnitude, V, at the secondary of
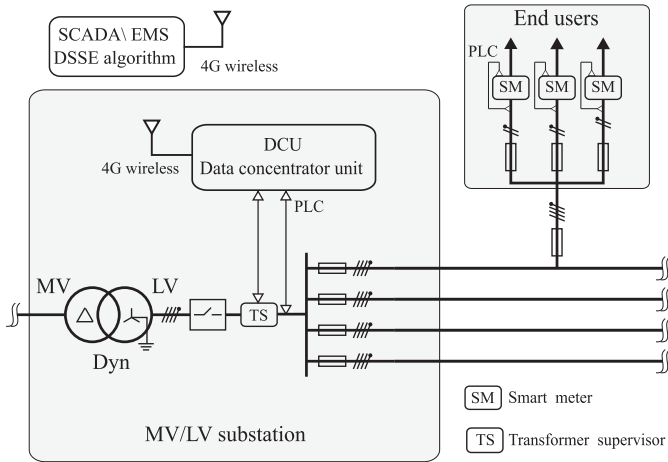
Fig. 2. Typical layout of a European LVDS.

the DT, measured by TS. This makes the network observable. Moreover, the level of redundancy is increased by adding the voltage measurements from SMs alongside with active and reactive power flow measurements (P_f, Q_f), from line supervisors at the low voltage side of the DT. This scenario makes it feasible to conduct DSSE downstream from the DT [10], and this is the approach considered in the present study. Both SM and TS instantaneous measurements are obtained through the DCU. As shown in Fig. 1, the request is conducted sequentially, alternating between a SM and the TS, until a cycle is completed after going through all the SMs. According to the above, DSSE is initiated once the system is observable, i.e. after the completion of the first full cycle. Then, the DSSE algorithm performs a new estimation each time a new couple of readings from a SM and TS is received by the DCU.

According to the measuring infrastructure considered in this study, which corresponds to a utility in the north of Spain, the DCU is located at the MV/LV substation, as illustrated in Fig. 2. The sequential nature of the data request is an inherent problem of the PLC technology. The casuistic here is very diverse: in DTs with a low number of customers, all data can be obtained in a time interval of 5 minutes; however, this time can be as high as 60 minutes in other scenarios. In the present case study, the time invested in making the request and receiving the data of a single SM can vary from 21 to 141 seconds with an average value of 45.56 seconds. The time delay for the TS measurement is a fixed parameter set at 15 seconds.

It is worth noting that the time-delayed SM measurements are inconsistent from the point of view of the DSSE due to their lack of synchronization. However, each SM measurement set (V, P_{inj}, Q_{inj}) or TS measurement set (V, P_f, Q_f), include simultaneous measurements.

III. DSSE METHODOLOGY

There are essential different features between the DS and transmission system. Thus, the DS has a higher R/X ratio and imbalances among phases, which lead to a higher level of complexity in the formulation of the SE problem. Also, there are constraints on the communication system, such as the network

bandwidth, which results in a limited rate of data exchange [20] and low availability of real-time measurements. This makes the use of TSSE techniques unsuitable for application to the DS [25]. The most common techniques used by distribution system estimators can be listed as follow [16], [26]:

1) WLS estimator.
2) LAV estimator.
3) WLAV estimator.
4) SHGM estimator.

Singh *et al.* [27] assessed the behaviour of WLS, WLAV and SHGM techniques. The outcome was that the WLAV and SHGM techniques cannot be applied directly to distribution networks and need considerable adjustment to get coherent and accurate results. The authors of this work concluded that WLS gives coherent and superior performance in distribution networks. The WLS estimator leads to a cohesive effectiveness performance under Gaussian hypothesis for recognized noise features [16].

Here, the implementation of DSSE algorithm is based on the WLS method. It is worth mentioning that the DSSE employed in this study is working online utilizing the instantaneous SM measurements and it is considered as a real-time application. Furthermore, the neutral voltage magnitude and angle at each bus are explicitly included in the vector of SV without any reduction, which is similar to the approach shown by one of the DSSE models introduced in [28]. The main adopted assumptions are:

1) An unbalanced 3-phase four wire system is considered, as the one shown in Fig. 2.
2) The loads are three phase or single phase considering that all measurements are recorded in a phase-to-neutral basis and all the electrical variables are expressed in per unit (pu).
3) Each measurement is affected by errors, which are statistically independent and can be described using a Gaussian probability distribution with zero mean and a standard deviation related to the technical characteristics of the measurement instrument [29].

In state estimation the general measurement model can be represented as

$$\mathbf{z} = \begin{bmatrix} z_1 \\ z_2 \\ \vdots \\ z_m \end{bmatrix} = \begin{bmatrix} h_1(x_1, x_2, \ldots, x_n) \\ h_2(x_1, x_2, \ldots, x_n) \\ \vdots \\ h_m(x_1, x_2, \ldots, x_n) \end{bmatrix} + \begin{bmatrix} e_1 \\ e_2 \\ \vdots \\ e_m \end{bmatrix} = \mathbf{h}(\mathbf{x}) + \mathbf{e}, \tag{1}$$

where $\mathbf{z}$ is the regular measurements vector, $\mathbf{x}$ is the SV which contains the angles and magnitudes of phase and neutral voltages w.r.t. ground, $\mathbf{h}(\mathbf{x})$ is the regular measurement functions vector where functions are built to cope with the actual field measurements, $\mathbf{e}$ is the error vector, m is the number of measurements and n is the number of state variables. According to the aforementioned assumptions, the covariance matrix is diagonal and the non-zero elements are the measurement variances, i.e.

$$cov(\mathbf{e}) = \mathbf{R} = diag\{\sigma_1^2, \sigma_2^2, \ldots, \sigma_m^2\}. \tag{2}$$

The estimation problem can be formulated as a Lagrangian function to minimize the objective function in (3) subjected to two equality constraints as in (4) and (5). Thus, the Lagrangian

function is written as in (6) [30],

$$J(\mathbf{x}) = \sum_{i=1}^{m} \frac{(z_i - h_i(\mathbf{x}))^2}{\mathbf{R}_{ii}} = [\mathbf{z} - \mathbf{h}(\mathbf{x})]^T \mathbf{R}^{-1} [\mathbf{z} - \mathbf{h}(\mathbf{x})],$$

(3)

$$\mathbf{c}(\mathbf{x}) = 0,$$

(4)

$$\mathbf{r} - \mathbf{z} + \mathbf{h}(\mathbf{x}) = 0,$$

(5)

$$\mathcal{L} = J(\mathbf{x}) - \lambda^T \cdot \mathbf{c}(\mathbf{x}) - \boldsymbol{\mu}^T \cdot (\mathbf{r} - \mathbf{z} + \mathbf{h}(\mathbf{x})),$$

(6)

where λ is the vector of Lagrange multipliers for virtual measurements, $\mathbf{c}(\mathbf{x})$ represents the non-linear functions relating virtual measurements with state variables such as those derived from zero-injection buses and from bus current balances and $\boldsymbol{\mu}$ is the vector of Lagrange multipliers for regular measurements. $\mathbf{r}$ is the residual vector, built with the differences between measured and estimated values of regular measurements. Using a flat-start and the Gauss–Newton's method, the states, $\mathbf{x}$, are iteratively estimated till the specified tolerance, which in this study is set to 10^{-5}.

$$\mathbf{x}_k = \mathbf{x}_{k-1} + \Delta\mathbf{x}_k$$

(7)

In (7), k is the iteration number. According to the augmented matrix approach [30], which shows a high immunity against ill-conditioning, the WLS problem is solved as follows,

$$\begin{bmatrix} \alpha^{-1}\mathbf{R} & \mathbf{H} & 0 \\ \mathbf{H}^T & 0 & \mathbf{C}^T \\ 0 & \mathbf{C} & 0 \end{bmatrix} \begin{bmatrix} \boldsymbol{\mu} \\ \Delta\mathbf{x} \\ \lambda \end{bmatrix} = \begin{bmatrix} \mathbf{z} - \mathbf{h}(\mathbf{x}) \\ 0 \\ -\mathbf{c}(\mathbf{x}) \end{bmatrix},$$

(8)

where,
- The coefficient matrix is called the Hachtel's matrix,
- $\mathbf{H}$ is the Jacobian of regular measurements,
- $\mathbf{C}$ is the Jacobian of virtual measurements,
- α is a scale factor used to improve the condition number of the Hachtel's matrix with no influence on the estimated state (it is selected in this work as the minimum variance of the set of regular measurement errors),

The SV, $\mathbf{x}$, consists of phase-to-ground and neutral-to-ground voltage phase angles and magnitudes at each bus, except for the voltage angle of phase a at the LV side of the DT, which is taken as a reference (i.e. it is considered as the slack bus). Notice that the neutral voltage magnitude and angle at the slack bus are also excluded from $\mathbf{x}$ as the DT is grounded at this point.

The set of measurements, $\mathbf{z}$, and their corresponding measurement functions, $\mathbf{h}(\mathbf{x})$, include phase-to-neutral voltage magnitudes and per-phase active and reactive power injections for SMs, and phase-to-neutral voltage magnitudes and per-phase active and reactive power flows for the TS located at the line connected to the secondary of the DT.

IV. PROPOSED APPROACH

A. Estimation of Voltage Phase Angles

According to the studies shown in [31] and [32], the traditional WLS faces a challenge to get accurate results, especially with regard to the estimation of voltage phase angles at phases b and c. To overcome this issue, the authors propose a modification in constructing the equality constraints by adding a new set for phase angle b and c as shown in (9). This formulation enables detecting the unbalance of phase angle b and c at the slack bus and permits the WLS algorithm to converge fast while getting the accurate solution. Although, the method presented in [32] achieved better results considering synchronized measurements of SM, its performance degrades in case of non-synchronized measurements assumption as will be discussed in Section V-D.

$$\mathbf{c}(\mathbf{x})_{\theta_b}^1 = \sum_{bus=1}^{B} (\cos\theta_b^{bus} - \cos\theta_{bb})$$

(9a)

$$\mathbf{c}(\mathbf{x})_{\theta_b}^2 = \sum_{bus=1}^{B} (\sin\theta_b^{bus} - \sin\theta_{bb})$$

(9b)

$$\mathbf{c}(\mathbf{x})_{\theta_c}^1 = \sum_{bus=1}^{B} (\cos\theta_c^{bus} - \cos\theta_{cc})$$

(9c)

$$\mathbf{c}(\mathbf{x})_{\theta_c}^2 = \sum_{bus=1}^{B} (\sin\theta_c^{bus} - \sin\theta_{cc})$$

(9d)

In (9), $\mathbf{c}(\mathbf{x})_{\theta_b}$ and $\mathbf{c}(\mathbf{x})_{\theta_c}$ are the new equality constraint functions for phase angle b and c, respectively. B is the number of buses within the network. θ_b^{bus} and θ_c^{bus} are the estimated phase angle b and c at each bus, respectively. θ_{bb} and θ_{cc} are constants for the default set angles of phase b and c at the slack bus, respectively.

B. Bad Data Detection

The ability to detect bad data depends mainly on the measurement set. The detection of bad data in unbalanced DSs is usually difficult due to the low measurement redundancy and the uncertainty of load models [33]. In general, the classic WLS DSSE is more sensitive to measurement noise and bad data, which may significantly affect the estimation results. In this method, the bad data detection and identification process is conducted after the estimation process. There are limited methods in the literature oriented to detect contaminated measurements with gross errors. The LNR test is one of them. Sometimes, the presence of measurement interaction can take place, which is mostly due to network topology, measurement location, and the weight assigned to each measurement. Considering the case of two or more interacting measurements containing conforming errors, the LNR test may fail to identify bad data.

Mahalanobis distance method is used to detect outliers; however, it is not suited for multiple outliers found at the same time. Certainly, as this method is based on non-robust statistics, a masking effect can take place when facing such a situation [34]. Hat matrix, K, is a known method to detect leverage points based on the use of diagonal elements of $\mathbf{H}$ by means of $K = \mathbf{H} \cdot (\mathbf{H}^T \cdot \mathbf{H})^{-1} \cdot \mathbf{H}^T$. However, it is prone to masking and swamping effects, as mentioned in [21]. Also, for a highly unbalanced DS, the calculation of $(\mathbf{H}^T \cdot \mathbf{H})^{-1}$ may lead to further ill-conditioning. In contrast, the robust estimators which utilize PS are suitable for online application and can detect multiple outliers and leverage points. These methods reduce the weight of bad measurements with a high residual during the

iterative estimation process, and thus, the negative impact of bad data on the estimation quality [34].

C. Modified Version of PS

In order to solve the inconsistent problem derived by the latency of the measurements of SM which may be considered as multiple bad data and since all the estimators, mentioned in Section III have limitations in detecting multiple bad data, a modified version of PS method [30] is implemented in the proposed DSSE algorithm to turn the DSSE algorithm into a robust one. PS is used in this implementation because it is robust to leverage points and multiple outliers at the cost of an increased computational effort.

The formula of PS for a specific measurement, i, presented in [21], [30] and [34], is shown in (10) and (11).

$$\text{PS}_i = \max_{\hat{H}_p} \frac{|\hat{H}_i^T \cdot \hat{H}_p|}{\beta} \quad \text{for} \quad p = 1, 2, \dots, m, \tag{10}$$

$$\beta = 1.1926 \cdot \text{med}_i\{\text{med}_{i \neq p}\{|\hat{H}_i^T \cdot \hat{H}_p + \hat{H}_p^T \cdot \hat{H}_p|\}\}, \tag{11}$$

where $\hat{H} = \mathbf{R}^{\frac{-1}{2}} \cdot \mathbf{H}$, which is the set of non zero row vectors of the weighted Jacobian matrix of regular measurements and med_i represents the median of the ith data-set. After computing PS_i, the weight factor ω_i for the ith measurement, is obtained as in (12),

$$\omega_i = \min \left\{ 1, \left[\frac{\chi^2_{v,0.975}}{\text{PS}_i} \right]^2 \right\}, \tag{12}$$

where $\chi_{v,0.975}$ is the Chi-square statistics for the ith measurement, v stands for the degrees of freedom (number of non-zero items in the ith row in the Jacobian matrix of regular measurements). w_i is used only in the right side of (14) as a condition and it is evaluated offline from the Jacobian matrix assessed at the flat start voltage profile to save computing time [34], [35].

To account for the short-term load variation that takes place because of OD, the measurement variances used in the proposed DSSE algorithm were calculated based on [10] as in (13). Furthermore, instead of using the w_i to update the ith measurement variance, a de-weighting factor, dWF_i, is adopted in this study. dWF_i is generated according to the OD concept introduced in [10], and it was found to be more effective to re-weight the measurements set (V_d, P_d, Q_d) of a specific SM_d in the same manner which yields better classification for the inconsistent measurements handled by DSSE. Thus,

$$\sigma^2_{i,total} = \sigma^2_{i,noise} + \sigma^2_{i,OD} \tag{13}$$

$$dWF_{i,k} = \begin{cases} \text{OD}_{i,k-1} & \text{if } |\frac{r_i}{\sigma_i \cdot \omega_i}| \leq tp \\ (1+y) \cdot \text{OD}_{i,k-1} & \text{otherwise}, \end{cases} \tag{14}$$

where $\sigma_{i,noise}$ is the standard deviation of the error of measurement device and $\sigma_{i,noise}$ is the standard deviation of the error of short-term load variation for the ith measurement. r_i is the residual of the ith regular measurement, tp is a tuning parameter which is to be specified by the users and is usually set as $1 < tp < 3$, k is the iteration number, y is a small incremental

scalar chosen so as $0 < y < 1$ and OD_i, in seconds, is the initial value of de-weighting factor calculated at the first iteration as in (15). In this study, tp and y are set to 1.5 and 0.5, respectively. $dWF_{i,k}$ is updated at each iteration according to (14) and then multiplied by the corresponding diagonal element of the original measurement covariance matrix to form the new variance as in (16). Finally, the updated value of $\mathbf{R}$ is used in (8) to reduce negative effect of the delayed measurements on estimation quality till the convergence is achieved.

$$\text{OD}_{i,0} = Ts - T_i, \tag{15}$$

$$\mathbf{R}_{ii,k} = \mathbf{R}_{ii,0} \cdot dWF_{i,k}, \tag{16}$$

where Ts is the timestamp of the last updated TS instantaneous measurement set prior to the execution of the DSSE algorithm and T_i is the timestamp of the instantaneous i^{th} measurement. Note that $\text{OD}_i = 1$ instead of zero in case of TS measurements, to prevent canceling the effect of their associated measurement noise variances.

D. Robustness of the Proposed Approach

As the proposed approach shares the main structure of the classic WLS DSSE algorithm, it has the same feature of numerical stability acquired by using the augmented matrix method. However, the main problem arises from the nature of time-delayed measurements. In the case of homogeneous measurements that belong to the same timestamp, the capability of the DSSE algorithm to converge to the global minimum is very high; however, this capability is limited in the case of time-delayed measurements. In the latter case, a local minimum can be obtained due to the high sensitivity of the voltage angles estimation to errors, for phase b and c [32]. Accordingly, this leads to an estimation of a different combination of phase b and c voltage angles, rather than the reference voltage phase angles. The proposed DSSE overcomes this problem by using the phase angle constraints introduced in IV-A.

Regarding the setting of the parameters presented in the proposal, the main concern is to avoid the ill-conditioned problem caused by the high condition number of the coefficient matrix, while letting the proposed DSSE algorithm to converge to an accurate feasible solution. The parameter tp controls the performance efficiency of the proposed DSSE algorithm according to the type of DS. If tp tends to zero, the proposed DSSE reduces to the generalized LAV estimator; conversely, if tp tends to infinity, the proposed DSSE becomes the classic WLS estimator. A good choice for tp is recommended to be a value in the range between 1 and 3 [34]. Furthermore, y is considered as a fine-tuning parameter to accelerate the process of convergence keeping into consideration that a higher value may be used in case of lower time-delay set-up and vice versa. It results that the better value for y is obtained as

$$y = \frac{\sum_{i=1}^{m} \text{OD}_{i,0}/m}{max(\text{OD}_{i,0})}, \tag{17}$$

employed for the set of time-delayed measurements, m, handled by the proposed DSSE algorithm in an estimation.

During the real-time application of the proposed algorithm, the initial guess of the state vector used to start the iterative
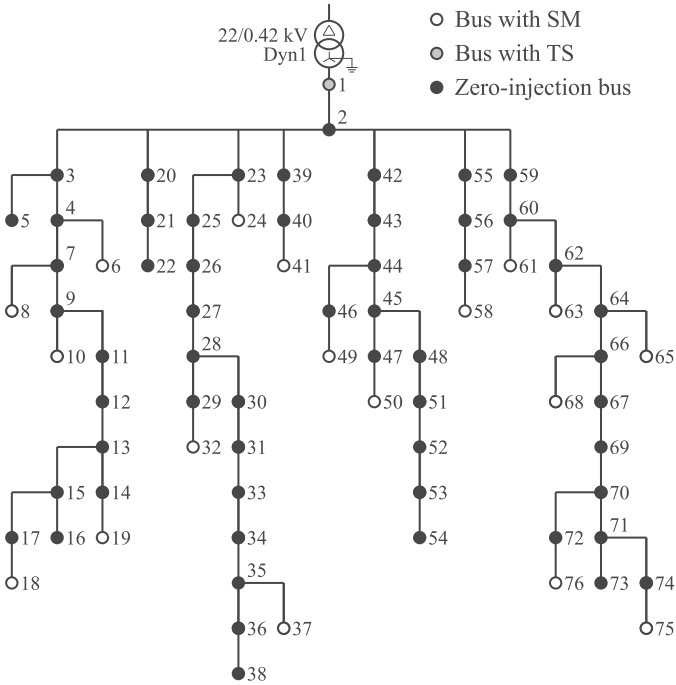
Fig. 3. Layout of the European LVDS used as a test bench.

Fig. 4. (a) Active and (b) reactive load profiles at bus 19, phase *c*, through a 24-hr period.

process is selected as the solution from the previous estimation, i.e. a flat profile is only selected for the first instant. This strategy has demonstrated an enhanced behaviour, leading to a lower number of iterations and further improving the probability of reaching convergence.

The proposal is considered as robust compared to the classic WLS. This is due to its capability to converge to an acceptable solution under a wide range of circumstances such as light and heavy unbalanced loads in presence of a diversity of distribution line lengths with different R/X ratios. It is worth noting that the proposed DSSE is working in this manner as a flexible and cost-effective tool through the PLC-AMI environment.

V. CASE STUDY

Three methods of DSSE are considered in this study for performance comparison: the first is the classic WLS algorithm mentioned in Section III, the second is the SyM-WLS method introduced in [32], and finally, the third is the proposed approach introduced in the present work. For the benefit of the reader, he is advised to read [32] regarding SyM-WLS method.

A. Network Description

An existing realistic European LVDS, illustrated in Fig. 3, is employed in this case study in order to test the validity of the proposed approach. The studied distribution network is grounded only at the low voltage (LV) side of the DT through a resistor. As mentioned in Section II, the study is conducted downstream from the LV side of the DT. The network consists of 7 feeders with a total length of 1.792 km and 76 buses with 4 nodes each for phases *a*, *b* and *c* and neutral. Furthermore, there are 54 single-phase SMs connected at phases *a*, *b* and *c* at 18 of the 76 buses. The SMs are located at residential loads
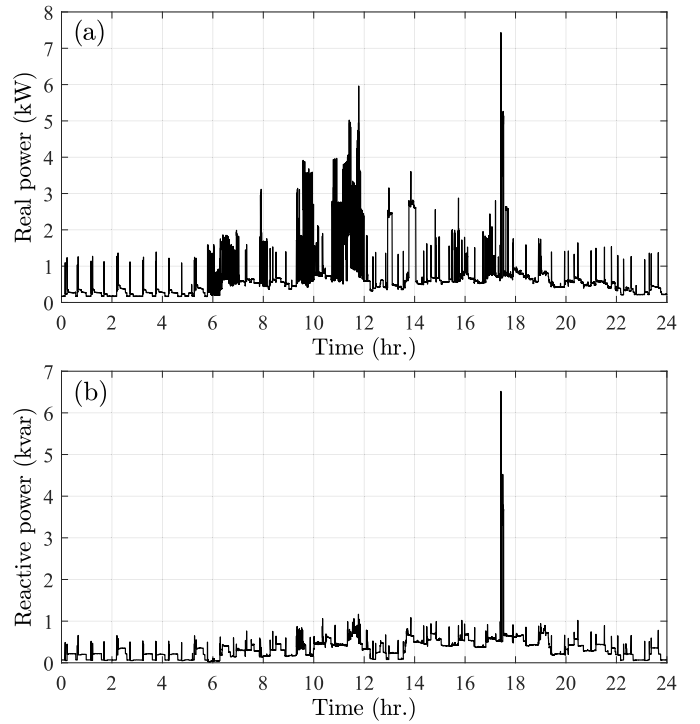
and their measurements are phase-to-neutral voltage magnitude and active and reactive power injections. Moreover, the TS provides the following measurements: phase-to-neutral voltage at the LV side of the DT and per-phase active and reactive power flow at the line connecting buses 1 and 2. The locations of SMs, TS and zero-injection buses are depicted in Fig. 3. For simplicity, it is assumed that there is no mutual coupling through phases and neutral wires, which is commonly accepted in this type of circuits. The load profiles, sampled at one second during a 24-hour period, are taken from an Austrian project named as ADRES-CONCEPT [36]. In order to simulate the measurement acquisition process, the topological information and load profiles are used by an unbalance power flow (PF) algorithm, verified by OpenDSS [37]. Thus, the true SVs of the network for each snapshot every second are calculated during a 24-hr period. As an example, the load profile at bus 19, phase *c*, is shown in Fig. 4.

The measurements from SMs and TS are obtained from the mentioned PF solution by adding Gaussian noise. The same set of measurement noise is applied for all methods in order to guarantee a fair comparison. According to [30], the standard deviations used to generate the noisy measurements are obtained as

$$\sigma = g \cdot \gamma \cdot \text{FS}, \quad (18)$$

where FS stands for the full scale of the measurement device, γ for its precision class and g is a number which depends on the type of measurement. The specific values used in this case study are addressed in Table I.
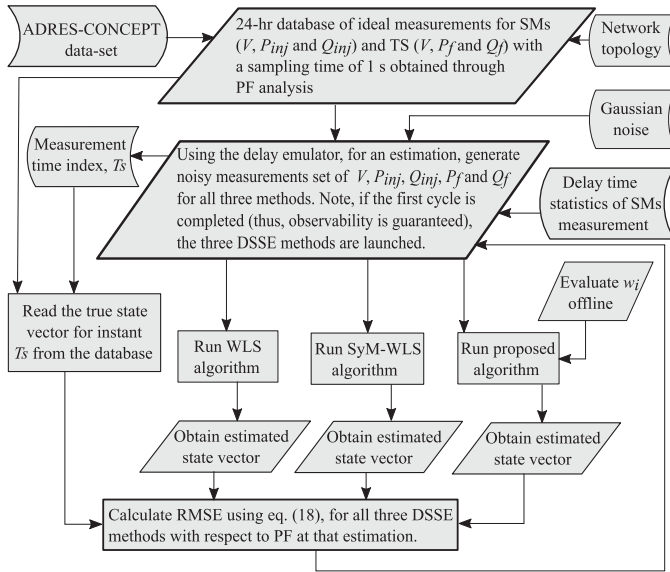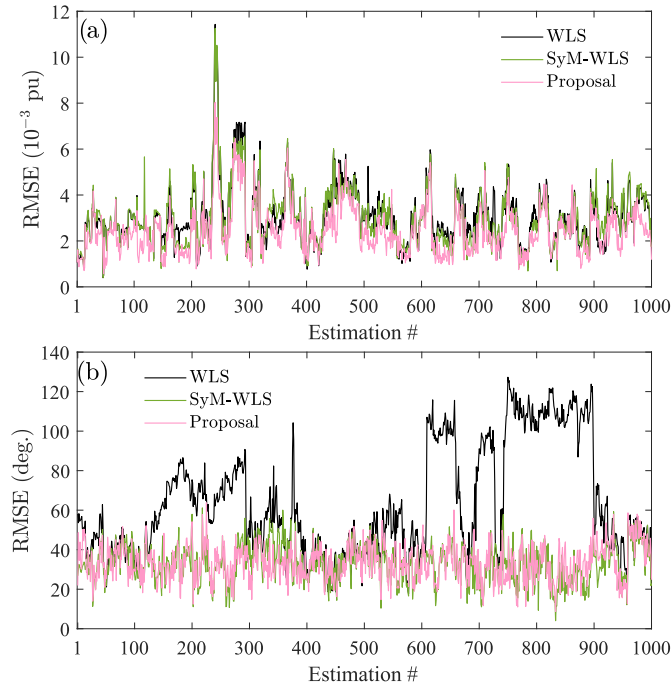
Fig. 5.   Flowchart of the DSSE process.

Fig. 6.   RMSE of the estimations offered by the different algorithms; a) for bus voltage magnitudes and, b) for bus voltage phase angles.
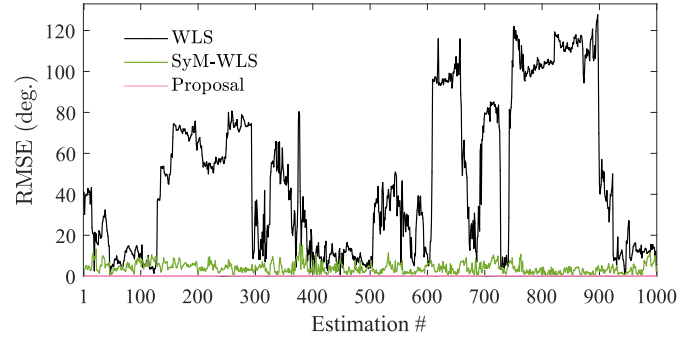

Fig. 7.   RMSE of the estimations offered by the different algorithms for bus voltage phase angles excluding the effect of the voltages at the neutral conductor.

TABLE I
MEASUREMENT NOISE PARAMETERS

	Voltages	Power injections	Power flows
$g \cdot \gamma$	0.001	0.005	0.005
Full scale	350 V	12 kW/kvar	15 kW/kvar
V_{base}/S_{base}	$400/\sqrt{3}$ V	10 kVA	10 kVA

The approaches of the three methods, described in Section III and IV, are kept the same except for the one proposed in this work. In the study presented in this section, OD_i in (15) is set to 1 and applied to all the measurement set. The first two bad measurements (P_{inj}, V) are obtained by dividing the corresponding actual measurements by 20 as it may happen with SM tampering. The third bad measurement (P_f) is obtained by multiplying the actual measurement by 20, which tries to emulate an error in the configuration of the scaling of a CT. The leverage point is identified if PS_i is greater than its cut-off (chi-squared) value as in (12) [34], which is illustrated in Table II.

It is worth mentioning that in case of the classic WLS method, the detection and identification of bad data are conducted only after the estimation process by processing the measurement residuals to define the LNR, [30]. The process starts by comparing the value of the objective function, $J(\mathbf{x})$, with a predefined threshold. If its value is greater than the threshold, the presence of bad data in the measurement set is assumed. In a second stage, the LNR is calculated to identify the bad measurement.

In fact, the DSSE algorithm is not suitable for an online implementation, as the calculation of the LNR is only carried out after the execution of the estimation algorithm. Moreover, in case of multiple bad measurements, their elimination should be done one by one. Furthermore, the LNR may fail to identify the bad measurement. Thus, the LNR is used directly, in this test, to check its effectiveness to identify bad measurements in the classic WLS and SyM WLS methods for comparison purpose. Through this test, its threshold is set to 3.

It can be seen from Table III that the proposal can deal with multiple bad measurements by down-weighting them resulting in the highest residuals. Although the other two methods can reduce the effect of bad data with a significant accuracy in case of a corrupted voltage measurement, they fail to attain the same behaviour with corrupted real power injection or power flow measurements. This is understandable, given that the latter

B. Bad Data Analysis

The main objective of this paper is to propose a model which can deal with the problem of time-delayed measurements of SMs. However, to highlight the effect of bad data measurements contaminated with gross errors on the proposed PS based model, synchronised measurements are assumed in this subsection. The measurement set, i.e. ($V, P_{inj}, Q_{inj}, P_f, Q_f$), is fed to the three DSSE methods. This measurement set is obtained from the PF solution by adding Gaussian noise to the result of this analysis. Three measurements are intentionally altered for the purpose of this study.
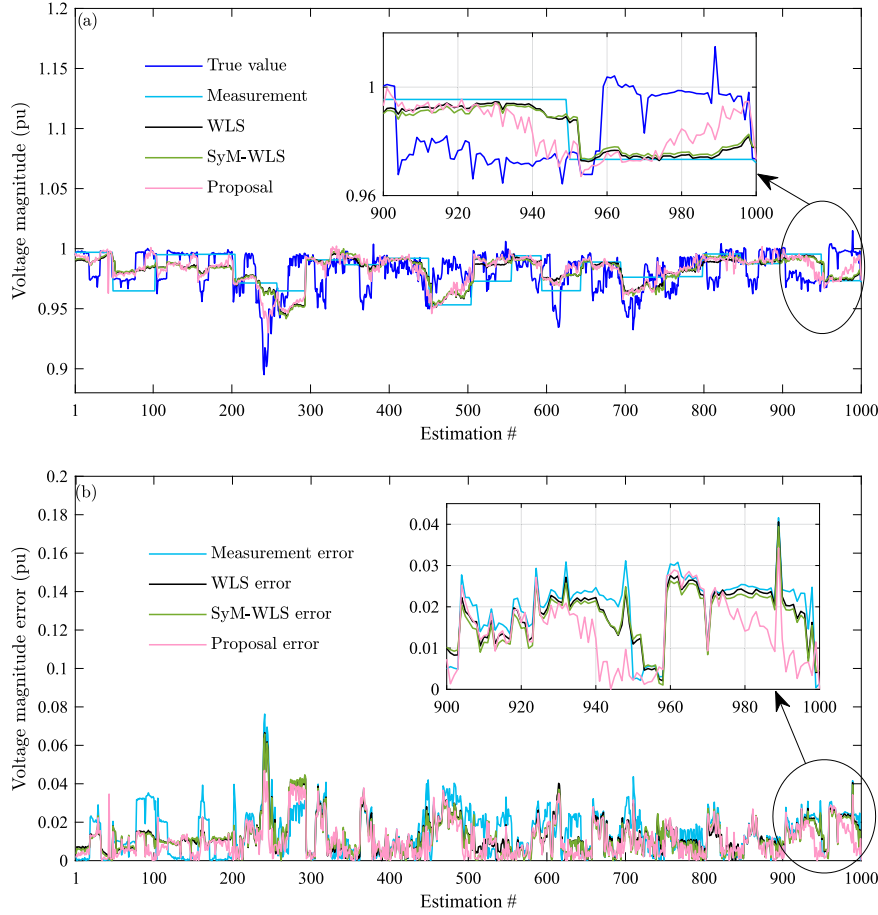
Fig. 8. Comparison of estimations derived from the different algorithms at a terminal bus (bus 75, phase *c*) using a typical load profile. (a) voltage magnitude, and (b) voltage magnitude error.

TABLE II
DETAILS OF BAD MEASUREMENTS WITH GROSS ERRORS

No.	Meas. type	Meas. location[a]	Actual meas. [kW/V]	Bad meas. [kW/V]	Bad meas. type defined by PS
1	P_{inj}	B37, Ph *a*.	−19.467	−0.973	Leverage
2	P_f	L1 (B1-B2), Ph *c*.	22.96/ − 8.437[*]	459.15/ − 168.73[*]	Leverage
3	V	B37, Ph *a*.	223.566	11.178	Outlier

[a]B: bus, L: line, Ph: phase.
[*]In case of SyM-WLS.

TABLE III
RESPONSE OF THE DIFFERENT METHODS TO BAD MEASUREMENTS

Meas.	Classic WLS Residual [kW/V]	Estimate [kW/V]	SyM-WLS Residual [kW/V]	Estimate [kW/V]	Proposal Residual [kW/V]	Estimate [kW/V]
P_{inj}	6.78	−7.75	6.33	−7.31	19.63	−20.58
P_f	8.95	450.2	−12.57	−156.16	434.1	25.06
V	−202.23	213.15	−215.09	226.24	−210.48	221.63

TABLE IV
PERFORMANCE COMPARISON OF THREE DSSE METHODS - TYPICAL LOAD
PROFILE

	Phase Voltage Magnitude MAE [pu]	AAE [pu]	Neutral Voltage Magnitude MAE [pu]	AAE [pu]
WLS	0.0322	0.0019	0.0443	0.0026
SyM-WLS	0.0302	0.0018	0.0594	0.0025
Proposal	0.0177	0.0013	0.0442	0.0024

	Phase Voltage Angle MAE [deg.]	AAE [deg.]	Neutral Voltage Angle MAE [deg.]	AAE [deg.]
WLS	179.81	36.43	179.998	72.06
SyM-WLS	25.05	3.05	179.997	50.33
Proposal	0.94	0.13	179.761	49.67

are low redundant measurements while the former is a high redundant measurement. Finally, the LNR only identifies a bad measurement properly in case of SyM-WLS, while the classic WLS misidentifies good measurements.

It is observed that the estimation results, obtained for the three methods through the bad data analysis described in this subsection, allow to conclude that none of the classic WLS

or SyM-WLS methods can match the phase angles *b* and *c* of the reference voltage with an acceptable accuracy. Conversely,
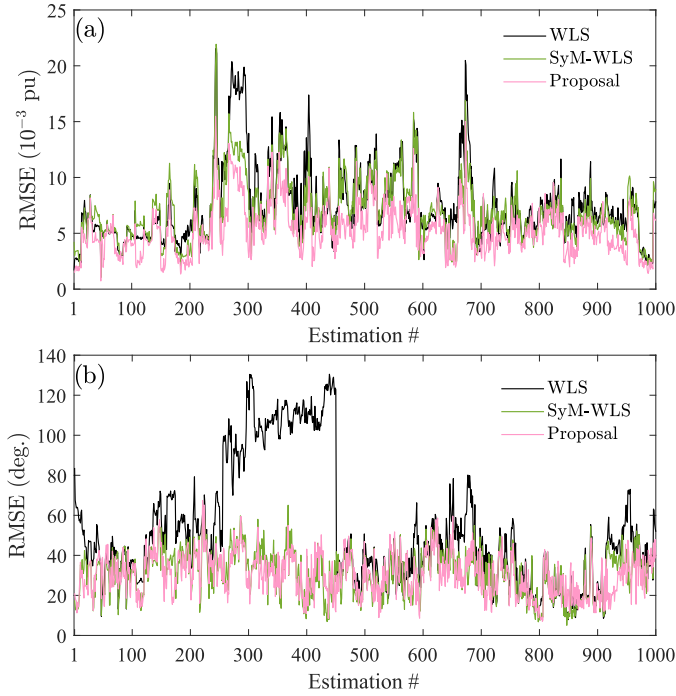
Fig. 9. RMSE of the estimations offered by the different algorithms; a) for bus voltage magnitudes and, b) for bus voltage phase angles.
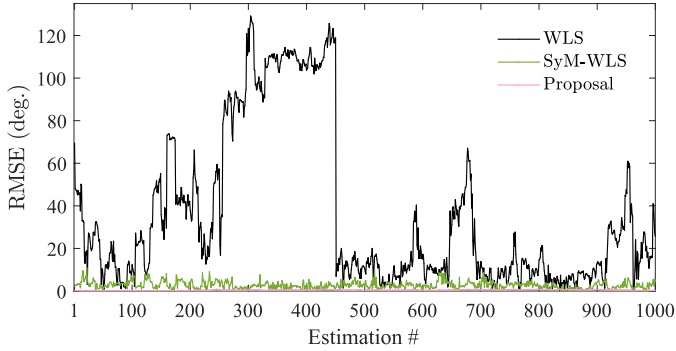

Fig. 10. RMSE of the estimations offered by the different algorithms for bus voltage phase angles excluding the effect of the voltages at the neutral conductor.

the method proposed in this work can trace these angles with reasonable precision and, at the same time, it accounts for the three-phase unbalance regarding the voltage phase angles. It is worth mentioning that the PS may fail in case of presence of two bad leverage measurements with opposite sign of respective coefficients, as masking takes place. Similarly, PS may fail if two good leverage points interacts in such a manner that their hat coefficients are of same sign, as swamping happens [21].

C. Delay Modelling

In order to model the real behavior of the communication delays linked to PLC technology, field data obtained from a pilot project conducted by the DSO in this grid is used. In the appendix, the real delays recorded for different samples of the SMs are represented against the distance from the SM to the DCU. A curve fitting method using an exponential equation as

TABLE V
PERFORMANCE COMPARISON OF THREE DSSE METHODS - SCALED LOAD PROFILE

	Phase Voltage Magnitude		Neutral Voltage Magnitude	
	MAE [pu]	AAE [pu]	MAE [pu]	AAE [pu]
WLS	0.0709	0.0054	0.0805	0.0057
SyM-WLS	0.0601	0.0048	0.0823	0.0055
Proposal	0.0450	0.0028	0.0788	0.0050
	Phase Voltage Angle		Neutral Voltage Angle	
	MAE [deg.]	AAE [deg.]	MAE [deg.]	AAE [deg.]
WLS	176.82	28.74	179.997	64.38
SyM-WLS	17.20	2.12	179.991	48.24
Proposal	1.91	0.37	179.853	45.26

in (19a) is used to obtain the expected delay of each device, Y_s. Two different curves, $s \in \{1, 2\}$, are obtained: a) to account for the case in which the injection phase at the DCU is the same as the phase where the SM is installed, $s = 1$, and b) to account for the case in which the injection is conducted at a different phase, $s = 2$. The so-called delay emulator built in this work does not directly use the delay predicted by this curve fitting method, Y_s. On the contrary, to prevent this delay from being fully deterministic, the standard deviation, STD_s, of the fitting process is obtained according to (19b). Thus, the emulator produces a random estimate of the time delay of each SM, Y_s^{est}, considering a Gaussian distribution of mean Y_s and standard deviation STD_s.

$$Y_s = a_s \cdot e^{(b_s \cdot dist)} \tag{19a}$$

$$STD_s = \sqrt{\frac{1}{N_s} \sum_{p=1}^{N_s} (TD_{s,p} - Y_{s,p})^2} \tag{19b}$$

In (19a), a_s and b_s are constants obtained from the curve fitting method. Their values are shown in the appendix. *dist* stands for the distance (in meters) from the SM to the DCU. The delay estimated by the curve fitting method, Y_s, is provided by this equation in seconds. In (19b), STD_s stands for the standard deviation of the fitting method, N_s for the number of samples and $TD_{s,p}$ and $Y_{s,p}$ for the actual (field data) and estimated delays (according to the curve fitting method) for each sample.

D. Simulation Results and Discussion

Through out this study, RMSE of the estimated SVs (i.e. the magnitude and angle of phase-to-ground and neutral-to-ground voltages), calculated as in (20), is set to be the main factor of evaluation. To capture the overall performance, the MAE and AAE are also considered.

$$\text{RMSE} = \sqrt{\frac{1}{N} \sum_{i=1}^{N} |x_i^{est} - x_i^{true}|^2}, \tag{20}$$

where N is the number of total nodes of the network under study (considering phases a, b, c and neutral), x_i^{est} is the estimated voltage magnitude in pu or angle in deg. and x_i^{true} is the true voltage magnitude in pu or angle in deg. obtained from the PF solution. Note that the RMSE is calculated each
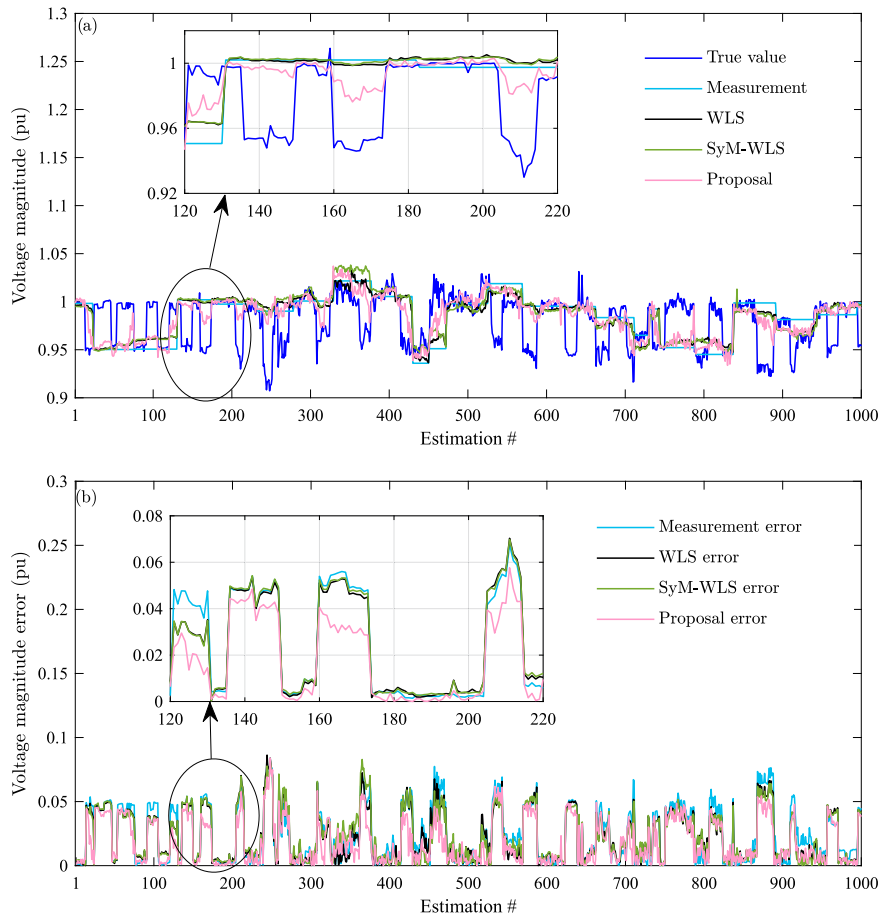
Fig. 11. Comparison of estimations derived from the different algorithms at a terminal bus (bus 37, phase *c*) using a peak-load highly unbalanced load profile. (a) voltage magnitude, and (b) voltage magnitude error.

time that the estimator produces a new output by assessing voltage magnitudes and angles separately. On the contrary, MAE and AAE are computed only once, separately for four value types, i.e. phase voltage magnitude, neutral voltage magnitude, phase voltage angle and neutral voltage angle, for the full set of estimation instances which amounts to 1000 in this case study.

For comparison purposes, the PF snapshot used to evaluate the alternative three DSSE methods at each instance corresponds to the timestamp of the last updated TS measurement received by the algorithms. The flowchart of the DSSE process conducted in this case study is depicted in Fig. 5. Note that Ts stands for the timestamp of the instant in which the DSSE is launched.

1) Typical Load Profile (Scenario I): In this scenario, the standard load profile from the data-set is used and a PF analysis is conducted to obtain the state variables and ideal measurements from the grid with a sample time of 1 s.

At each estimation instance, the corresponding measurements, according to the output of the delay emulator and after the addition of Gaussian noise, are fed into the three DSSE algorithms under test, i.e. WLS, SyM-WLS and the proposal. The performance of these algorithms, assessed considering the first 1000 estimation instances (which covers a time span of around 22.7 hr.) through the RMSE is shown in Fig. 6(a) and Fig. 6(b) for voltage magnitude and voltage phase angle, respectively.
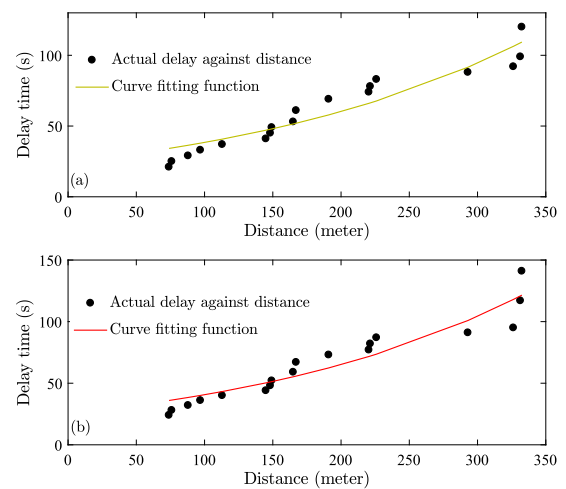

Fig. 12. Curve fitting functions of SM time delays and distance to the DCU. (a) for SMs installed at the same phase used for the signal injection and, (b) for SMs installed at phase different from the one used for the signal injection.

The other figures of merit, calculated over the said time span, are presented in Table IV.

As it can be seen from Fig. 6(a), a significant accuracy improvement of voltage magnitude estimation is achieved by

the proposal compared to both classic WLS and SyM-WLS. Furthermore, the maximum and average errors of voltage magnitude, illustrated in Table IV, bear witness to this improvement. Moreover, according to Fig. 6(a) and Table IV, SyM-WLS enhances the estimation accuracy of both phase and neutral voltage magnitudes compared to classic WLS. Furthermore, during most estimations, WLS has poor voltage magnitude estimation compared to both SyM-WLS and proposal. Meanwhile, the proposal is achieving the best performance over most estimations. Also, according to Table IV, the maximum and average errors offered by the proposal show the lowest values regarding both phase and neutral voltage magnitude versus classic WLS and SyM-WLS. This fact confirms the significant accuracy improvement of the estimation achieved by the current proposal.

With regard to the comparison of the WLS method with the current proposal, Fig. 6(b) highlights a significant estimation improvement of voltage phase angles when both phase voltages and neutral voltages are considered. On the contrary, those results are similar to the ones offered by the SyM-WLS algorithm. It is interesting to point out that, if the phase angles of neutral voltages are excluded from the calculation of the RMSE index, as illustrated in Fig. 7, the current proposal clearly outperforms the other two methods. The increase in the accuracy of the estimation of phase angles of phase voltages is due to the proposed equality constraints shown in (9). Notice that, according to Table IV, the accuracy of the estimation of phase angles of neutral voltages is also slightly improved with the current proposal. However, significant errors can still be present in the latter case due to the low magnitude of neutral voltages at certain buses.

In short, the new equality constraints, (9), lead to a clear improvement of the phase angle estimation of phase voltages. Meanwhile, the PS method is the main responsible of the improvement in the estimation of voltage magnitudes. In order to assess the quality of the improvements, Fig. 8(a) shows the phase-to-neutral voltage magnitude of the terminal bus 75 at phase c, along a set of 1000 estimations, which roughly comprises a time span of 22.7 hours. The results from the new proposal are compared in this figure with the ones derived from the WLS and SyM-WLS methods and depicted together with the true values obtained from the PF analysis and with the latest available measurement. The zoomed window in Fig. 8(a) clearly states that the new proposal shows the closest estimation to the true voltage profile; this is certainly confirmed by Fig. 8(b), which depicts the voltage estimation errors.

2) Scaled Load Profile (Scenario II): In order to test the performance of WLS, SyM-WLS and the current proposal under critical conditions, the scenario shown in V-D1 has been altered to emulate a peak-load case, in which voltage drops and neutral voltages are magnified. Thus, the active and reactive power profiles of the loads used in V-D1 have been scaled according to

$$P_{im,o}^{scaled} = f \cdot P_{im,o}^{typical}, \tag{21a}$$

$$Q_{im,o}^{scaled} = f \cdot Q_{im,o}^{typical}, \tag{21b}$$

where P and Q are the real and reactive power demand, respectively, im is the SM number, o is the time index and f is a scalar which is equal to 3.5 in case of phase a, 4.5 in case of phase b and 2 in case of phase c. These scalars are chosen to achieve a

clear unbalance of the grid, while avoiding to exceed operational constraints.

In the same way as in the previous scenario, the RMSE for voltage magnitudes and phase angles are depicted in Fig. 9 a and Fig. 9 b, respectively. The rest of the figures of merit are summarized in Table V. It can be concluded from Fig. 9 a, that the performance quality of the proposal in estimating voltage magnitudes is preserved. Even though the RMSE values are higher for all the methods assessed in this work, the overall profile is similar to the one obtained in the typical load scenario, with the proposed method showing always the smallest values. Moreover, the estimation of phase angles for phase and neutral bus voltages shows again a similar performance in the new proposal and in the SyM-WLS method, always improving the results of the classic WLS algorithm. This achievement, which is highlighted in Fig. 9 b, is due to the use of the new set of phase angle constraints, (9), in the proposal, and to the use of synthetic measurements in the SyM-WLS algorithm. The performance of the three methods are also clearly illustrated through Table III, which demonstrates the superiority of the new proposal.

Similarly to the case shown in V-D1, in the new scenario, if the estimation of the phase angle of neutral voltages are excluded from the calculation of RMSE, the superiority of the new proposal becomes more evident. This is clearly illustrated in Fig. 10. On the other hand, the estimation of the phase angles of neutral voltage for the scaled load profile becomes slightly more accurate than the ones obtained using the WLS or SyM-WLS alternatives. The MAE and AAE shown in Table V ensures the validity of the proposal against the classic WLS and SyM-WLS algorithms. Although in this case the values of MAE and AAE for voltage magnitudes are higher than the ones obtained for the typical load scenario, the performance of the proposal proves to be consistently superior than the other alternatives. Admittedly, the benefit of the proposal in terms of MEA and AAE is only marginal for the case of the estimation of neutral voltage magnitudes and phase angles.

In order to verify the validity of the proposal in case of the scaled load profile, Fig. 11 a depicts the estimations of the phase-to-neutral voltage magnitude at one specific terminal bus (bus 37, phase c) for the three alternative DSSE algorithms. For the sake of comparison, the true value of these measurements, obtained through PF analysis, are also represented in this figure together with the last available measurements. The zoomed window in Fig. 11 a, clearly points out that the current proposal outperforms the other methods in tracking the true value of the system. The zoomed window in Fig. 11 b confirms the proficiency of the proposal by representing the estimation errors derived from the different alternatives.

3) Different Set-Ups of Time-Delay: Apart from the two scenarios above, an additional simulation is carried out to figure out the impact of different delay set-ups on the estimation quality of the proposal. Thus, the proposal is evaluated by increasing/decreasing the original delays by $\pm 50\%$. This test is conducted exclusively for the heavy loaded case (scaled load profile) and not for the typical one, as the effect is magnified in the former case. Based on the additional simulation, it is observed that the performance of the proposal is almost stable considering the higher and lower set-up of the time delays.

Moreover, it can be noticed that, the other two methods (classic WLS and SyM-WLS) show a random performance, in which convergence within the specified tolerance is not guaranteed.

It is worth mentioning that the evolution of the de-weighting process in the proposed method may rarely result in an ill-conditioned problem, leading to divergence in a limited number of estimations. According to the whole study, to achieve more than 1000 successful estimation instances, less than 5 cases of non-convergence were obtained.

VI. CONCLUSION AND FUTURE WORK

This paper discusses the problem of real-time DSSE in European-type four-wire LVDSs with AMI based on PLC. The negative impact of PLC is due to its high latency and a sequential data sampling process. This in turn, results in poor estimation results. This work proposes a solution that allows the estimation of the state of the low voltage network with a reasonable accuracy considering the low quality of the measurements provided by the deployed infrastructure.

The proposal improves the estimation accuracy and achieves a better performance accredited by the results of two scenarios, one corresponding to a typical load profile and the other to a peak-load highly unbalanced case. The results validate the proposal by demonstrating a significant improvement compared to the classic WLS and SyM-WLS algorithms.

Further investigations are still required in order to upgrade the estimation accuracy of the neutral voltages, in both magnitude and phase angle. Moreover, the effect of the specific SMs reading sequence used by the DCU and its impact on the quality of DSSE algorithms should also be addressed in future works. Finally, a field implementation of the proposal would be desired to test its effectiveness in real conditions.

APPENDIX
PARAMETERS OF CURVE FITTING METHOD

The WLS method was used to fit (19a) to the experimental results in delay modeling. It is worth mentioning that, even though only a small part are shown in Fig. 12, around 800 real samples were used with this aim for each curve. Most of the samples from the same SM are similar, which strengthens the assumption of linking the delay of each SM with features such as its distance to DCU and its relation with the signal injection phase.

The parameters obtained for those SMs installed at the same phase used for the signal injection are

$$a_1 = 24.51; b_1 = 0.004498,$$

and the parameters obtained for the SMs installed at a different phase are

$$a_2 = 25.4; b_2 = 0.004708.$$

REFERENCES

[1] F. C. Schweppe and J. Wildes, "Power system static-state estimation, Part I: Exact model," *IEEE Trans. Power App. Syst.*, vol. PAS-89, no. 1, pp. 120–125, Jan. 1970.

[2] J. Chen, H. Chung, C. Wen, W. Li, and J. Teng, "State estimation in smart distribution system with low-precision measurements," *IEEE Access*, vol. 5, pp. 22713–22723, 2017.

[3] C. Alaton and F. Tounquet, "Benchmarking smart metering deployment in the EU-28," European Commission, Directorate-General for Energy, final report. Publications Office; 2020. doi: 10.2833/492070

[4] A. Alimardani, S. Zadkhast, J. Jatskevich, and E. Vaahedi, "Using smart meters in state estimation of distribution networks," in *Proc. IEEE PES Gen. Meeting*, 2014, pp. 1–5.

[5] M. Degefa, R. J. Millar, M. Koivisto, M. Humayun, and M. Lehtonen, "Load flow analysis framework for active distribution networks based on smart meter reading system," *Engineering*, vol. 5, pp. 1–8, 2013.

[6] F. Ni, P. H. Nguyen, J. F. G. Cobben, H. E. van den Brom, and D. Zhao, "Uncertainty analysis of aggregated smart meter data for state estimation," in *Proc. IEEE Int. Workshop Appl. Meas. Power Syst.*, 2016, pp. 1–6.

[7] I. Golub, E. Boloev, and Y. Kuzkina, "Using smart meters for checking the topology and power flow calculation of a secondary distribution network," *E3S Web Conf.*, vol. 139, pp. 1–5, 2019. [Online]. Available: https://doi.org/10.1051/e3sconf/201913901059

[8] T. N. Le, W. Chin, D. K.Truong, and T. H. Nguyen, "Advanced metering infrastructure based on smart meters in smart grid," in *Smart Metering Technol. and Serv.*, M. Eissa, Ed. Rijeka: IntechOpen, 2016, ch. 3. [Online]. Available: https://doi.org/10.5772/63631

[9] M. Kemal, R. Sanchez, R. Olsen, F. Iov, and H.-P. Schwefel, "On the trade-off between timeliness and accuracy for low voltage distribution system grid monitoring utilizing smart meter data," *Int. J. Elect. Power Energy Syst.*, vol. 121, pp. 1–9, 2020.

[10] A. Alimardani, F. Therrien, D. Atanackovic, J. Jatskevich, and E. Vaahedi, "Distribution system state estimation based on nonsynchronized smart meters," *IEEE Trans. Smart Grid*, vol. 6, no. 6, pp. 2919–2928, Nov. 2015.

[11] K. Samarakoon, J. Wu, J. Ekanayake, and N. Jenkins, "Use of delayed smart meter measurements for distribution state estimation," in *Proc. IEEE Power Energy Soc. Gen. Meeting*, 2011, pp. 1–6.

[12] T. C. Xygkis, G. D. Karlis, I. K. Siderakis, and G. N. Korres, "Use of near real-time and delayed smart meter data for distribution system load and state estimation," in *Proc. MedPower*, 2014, 2014, pp. 1–6.

[13] M. Hojabri, U. Dersch, A. Papaemmanouil, and P. Bosshart, "A comprehensive survey on phasor measurement unit applications in distribution systems," *Energies*, vol. 12, no. 23, 2019, Art. no. 4552.

[14] M. Asprou and E. Kyriakides, "The effect of time-delayed measurements on a PMU-based state estimator," in *Proc. IEEE Eindhoven PowerTech*, 2015, pp. 1–6.

[15] J. Liu, J. Tang, F. Ponci, A. Monti, C. Muscas, and P. A. Pegoraro, "Trade-offs in PMU deployment for state estimation in active distribution grids," *IEEE Trans. Smart Grid*, vol. 3, no. 2, pp. 915–924, Jun. 2012.

[16] A. Abdel-Majeed and M. Braun, "Low voltage system state estimation using smart meters," in *Proc. 47th Int. Universities Power Eng. Conf.*, 2012, pp. 1–6.

[17] A. Abdel-Majeed, S. Tenbohlen, D. Schöllhorn, and M. Braun, "Development of state estimator for low voltage networks using smart meters measurement data," in *Proc. IEEE Grenoble Conf.*, 2013, pp. 1–6.

[18] M. Cramer, P. Goergens, F. Potratz, A. Schnettler, and S. Willing, "Impact of three-phase pseudo-measurement generation from smart meter data on distribution grid state estimation," in *Proc. 23rd Int. Conf. Exhib. Electricity Distrib.*, 2015, pp. 1–5.

[19] R. Sanchez, F. Iov, M. Kemal, M. Stefan, and R. Olsen, "Observability of low voltage grids: Actual DSOs challenges and research questions," in *Proc. 52nd Int. Universities Power Eng. Conf.*, 2017, pp. 1–6.

[20] K. Dehghanpour, Z. Wang, J. Wang, Y. Yuan, and F. Bu, "A survey on state estimation techniques and challenges in smart distribution systems," *IEEE Trans. Smart Grid*, vol. 10, no. 2, pp. 2312–2322, Mar. 2019.

[21] C. S. Kumar, K. Rajawat, S. Chakrabarti, and B. C. Pal, "Robust distribution system state estimation with hybrid measurements," *IET Gener., Transmiss. Distrib.*, vol. 14, no. 16, pp. 3250–3259, 2020.

[22] P. Arsenio, M. Silva, D. Ribeiro, R. Barros, and P. Nunes, "Assessment of smart meter communication over PLC prime in a laboratory simulating a real grid," in *Proc. 25th Int. Conf. Electricity Distrib.*, 2019, pp. 1–4.

[23] M. S. Kemal, R. L. Olsen, and H. Schwefel, "Optimized scheduling of smart meter data access: A parametric study," in *Proc. IEEE Int. Conf. Commun., Control, Comput. Technol. Smart Grids*, 2018, pp. 1–6.

[24] M. T. Chaves, R. S. Barbosa, and L. Amorim, "Smart metering communication performance analysis in EDP distribuição," in *Proc. Ljubljana Workshop, Ljubljana, Slovenia (CIRED 2018)*. AIM, 2018.

[25] F. Ahmad, A. Rasool, E. Ozsoy, R. Sekar, A. Sabanovic, and M. Elitaş, "Distribution system state estimation-a step towards smart grid," *Renewable Sustain. Energy Rev.*, vol. 81, pp. 2659–2671, 2018.

[26] S. Kamireddy, N. N. Schulz, and A.K. Srivastava, "Comparison of state estimation algorithms for extreme contingencies," in *Proc. 40th North Amer. Power Symp.*, 2008, pp. 1–5.

[27] R. Singh, B. Pal, and R. Jabr, "Choice of estimator for distribution system state estimation," *IET Gener., Transmiss. Distribution*, vol. 3, no. 7, pp. 666–678, 2009.

[28] Y. Liu, J. Li, and L. Wu, "State estimation of three-phase four-conductor distribution systems with real-time data from selective smart meters," *IEEE Trans. Power Syst.*, vol. 34, no. 4, pp. 2632–2643, Jul. 2019.

[29] F. Adinolfi, F. Baccino, F. D'Agostino, S. Massucco, M. Saviozzi, and F. Silvestro, "An architecture for implementing state estimation application in distribution management system (DMS)," in *Proc. IEEE PES ISGT Europe*, 2013, pp. 1–5.

[30] A. Abur and A. G. Exposito, *Power System State Estimation: Theory and Implementation*. CRC Press, 2004.

[31] A. L. Langner and A. Abur, "Formulation of three-phase state estimation problem using a virtual reference," *IEEE Trans. Power Syst.*, vol. 36, no. 1, pp. 214–223, Jan. 2021.

[32] J. M. Cano, P. Arboleya, M. Rashad Ahmed, M. R. R. Mojumdar, and G. A. Orcajo, "Improving distribution system state estimation with synthetic measurements," *Int. J. Elect. Power Energy Syst.*, vol. 129, pp. 1–6, 2021.

[33] A. Primadianto and C. N. Lu, "A review on distribution system state estimation," *IEEE Trans. Power Syst.*, vol. 32, no. 5, pp. 3875–3883, Sep. 2017.

[34] L. Mili, M. G. Cheniae, N. S. Vichare, and P. J. Rousseeuw, "Robust state estimation based on projection statistics [of power systems]," *IEEE Trans. Power Syst.*, vol. 11, no. 2, pp. 1118–1127, May 1996.

[35] R. C. Pires, L. Mili, and F. A. B. Lemos, "Constrained robust estimation of power system state variables and transformer tap positions under erroneous zero-injections," *IEEE Trans. Power Syst.*, vol. 29, no. 3, pp. 1144–1152, May 2014.

[36] A. Einfalt "Konzeptentwicklung fr ADRES - Autonome Dezentrale Erneuerbare Energie Systeme," FFGForschungsprojekt, Energie der Zukunft, 1. AS, Projektnummer: 815674, Endbericht, Wien, 2011. [Online.] Available: https://www.ea.tuwien.ac.at/projects/adres_concept/EN/

[37] R. C. Dugan and D. Montenegro, "Open distribution system simulator (OpenDSS): Reference guide," in *Elect. Power Res. Inst.*, Jun. 2019. [Online.] Available: https://sourceforge.net/p/electricdss/wiki/Home/

Mahmoud Rashad Ahmed received the M.Sc. degree in electrical and control engineering from the Arab Academy for Science, Technology and Maritime Transport, Alexandria, Egypt, in 2014. He is currently working toward the Ph.D. degree in electrical and electronic engineering with the University of Oviedo, Oviedo, Spain.

He was an operation and maintenance Senior Electrical Engineer with EMC, MIDOR Oil Refinery, Egypt. His research interests include state estimation, distribution system modeling, smart grid operation, theft detection and localization in smart grids, and optimization algorithms in distribution systems.

José M. Cano (Senior Member, IEEE) received the M.Sc. and Ph.D. degrees in electrical engineering from the University of Oviedo, Oviedo, Spain, in 1996 and 2000, respectively.

In 1996, he joined the Department of Electrical Engineering, University of Oviedo, where he is currently a Full Professor. During 2012 and 2014, he was a Visiting Associate Professor with the Department of Electrical and Computing Engineering, The University of British Columbia, Canada, Vancouver, BC, Canada. His main research interests include power quality solutions for industry, power converters, power system state estimation, distributed generation, and smart grids.

Pablo Arboleya (Senior Member, IEEE) received the M.Sc. and Ph.D. (Hons.) degrees in electrical engineering from the University of Oviedo, Gijón, Spain, in 2001 and 2005, respectively.

He is currently an Associate Professor with the Department of Electrical Engineering, University of Oviedo. He holds the Gijón Smart Cities Chair with the University of Oviedo. His current research interests include microgrid and smart grid modeling and operation, applications of internet of energy, simulation of railway traction networks, and combined AC/DC power flow algorithms. He is the Managing Editor of the *International Journal of Electrical Power and Energy Systems* and the co-founder of Plexigrid.

Lucía Suárez Ramón received the M.Sc. degree in electrical engineering in 1997 from the University of Oviedo, Gijón, Spain, where she is currently working toward the Ph.D. degree with LEMUR Research Group.

She is also the Director of Smart Grid Operation with EDP. Her main research interests include the smart operation of terminal distribution networks, networks analysis and simulation, and failures detection.

Almoataz Y. Abdelaziz (Senior Member, IEEE) received the B.Sc. and M.Sc. degrees in electrical engineering from Ain Shams University, Cairo, Egypt, in 1985 and 1990, respectively, and the Ph.D. degree in electrical engineering according to the channel system between Ain Shams University, and Brunel University, Uxbridge, U.K., in 1996.

Since 2007, he has been a Professor of electrical power engineering with Ain Shams University. He has authored or coauthored more than 450 refereed journal and conference papers, 35 book chapters, and six edited books with Elsevier, Springer and CRC Press. In addition, he has supervised more than 80 master's and 35 Ph.D. theses. He is the Chair of the IEEE Education Society chapter in Egypt. He is the Editor of the *Electric Power Components and Systems Journal*, an Editorial Board Member, an Editor, an Associate Editor, and an Editorial Advisory Board member for many international journals. His research interests include the applications of artificial intelligence, evolutionary and heuristic optimization techniques to power system planning, operation, and control.